Research Square

Preprints are preliminary reports that have not undergone peer review.
They should not be considered conclusive, used to inform clinical practice,
or referenced by the media as validated information.

# Computational evaluation of anticancer potential of Pleurotus sajor caju derived bioactive compounds against breast cancer targets using virtual screening

**Supriya Maurya**
University of Allahabad
**Ravi Shanker**
University of Allahabad
**Adarsh Kumar Shukla**
Dr. Bhimrao Ramji Ambedkar Government Medical College, Kannauj Uttar Pradesh
**Saba Ehsan**
University of Allahabad
**Mohan P. Singh**
mpsingh.16@gmail.com
University of Allahabad

**Research Article**

**Keywords:** Breast Cancer, Pleurotu sajor-caju, Molecular docking simulations, Root mean square fluctuations (RMSF)

**Posted Date:** March 20th, 2026

**DOI:** https://doi.org/10.21203/rs.3.rs-9050350/v1

**License:** This work is licensed under a Creative Commons Attribution 4.0 International License. Read Full License

**Additional Declarations:** No competing interests reported.

## Abstract

Breast cancer remains a major global health challenge, with nearly 2.3 million new cases diagnosed each year. Pleurotus sajor-caju, a nutritionally rich mushroom, contains diverse bioactive constituents—including polysaccharides, terpenoids, and phenolic compounds—recognized for their anticancer potential. This study attempts to identify and prioritize key hub proteins involved in breast cancer progression and to screen potent inhibitory compounds derived from this mushroom. Protein–protein interaction analysis highlighted ten crucial targets, including CDKN2A, ERBB2, BRCA1, TP53, ESR1, CDH1, EGF, PTEN, EGFR, and MYC. Molecular docking and dynamic simulations further revealed two promising, orally active molecules-ethyl iso-allocholate and benzyl butyl phthalate—showing strong binding affinities and inhibitory potential comparable to standard drugs such as capecitabine and veliparib. ADMET profiling indicated favourable pharmacokinetic and safety attributes. Overall, the findings support advancing these mushroom-derived compounds to in-vitro and clinical evaluations for breast cancer therapy.


## 1. Introduction

Breast cancer is the most common tumor diagnosed in women worldwide and is a global health concern. Breast cancer accounts for about 2.3 million of the estimated 19.3 million new cancer diagnoses, and the incidence is still rising quickly [1].With particular focus to carriers and young women aged 49 and under who have a 2.1 risk of invasive breast cancer of germline BRCA1 or BRCA2 mutations, which are the most common hereditary gene mutations in this tumor, who are 40–80% more likely to get breast cancer in their lifetime [2][3]. Although successful multimodal medicines have led to a dramatic drop in mortality rates, cancer is still the second leading cause of death for women in the US [1].

Classifying breast cancer into its distinct subtypes is therefore essential for therapeutic decision-making and individual treatment. Luminal A, Luminal B, HER2 overexpression, basal, and normal-like tumors are among the five intrinsic subgroups of breast cancer [4]. The two primary biological processes that the Luminal A and Luminal B subtypes are known to express are proliferation/cell cycle and luminal/hormone-regulated pathways [4]. This sets them apart from other subtypes. Similar to the basal-like subtype, the HER2 enriched subtype is distinguished by the overexpression of genes and proteins linked to HER2 and proliferation [4]. For at least 70% of individuals with breast cancer, oestrogen receptor a (ERα), a member of most nuclear receptor types, has been identified as the primary internal cause of the disease; these patients are known as ER positive (ER+) [5][6]. Tamoxifen, and raloxifene which are selective estrogen receptor modulators (SERMs) that rival with estradiol for binding with ERα in breast tissue are mostly used for the remedy of $ER^+$ breast cancer [7]. Novel medication discovery is difficult, costly, and time-consuming because clinical trials have a relatively low approval rate. Many pharmaceutical companies are working on the de novo process, which takes about 14 years and costs 800 million dollars to discover a new medication [8] [9].

One possible method for finding new indications for a particular condition is drug repurposing (DR), which involves employing licensed medications (existing pharmaceuticals) [10]. One important method for confirming drug-target structure binding performance in computational drug repurposing procedures is molecular docking studies. Accurately identifying the disease's key genes (KGs) and targets with potential medications is crucial for diagnosis, prognosis, and treatment [11]. Among the most popular methods for disease-guided key gene identification is the analysis of gene expression profiles. Utilising gene expression patterns, we used several datasets collected from diverse situations to identify more common and stable BC-guided KG [7].

One of the primary edible species grown in Brazil, *P. sajor-caju*, commonly known as oyster mushroom or Houbitake, is a macroscopic, aerobic fungus that is a member of the genus Pleurotus and family *Pleurotaceae* [12]. It accounts for 17% of the country's yearly mushroom production. Interestingly, there are currently over 14,000 known kinds of mushrooms, and another 126,000 species have not yet been found [13]. *P. sajor-caju* has been linked in studies to high nutritional content, bioactive chemicals, and medicinal qualities such as anti-inflammatory, anti-diabetic, anti-bacterial, anti-fungal, anti-parasitic, anti-hypertensive, anti-cancer and antiviral effects [14] [15]. Numerous secondary metabolites and bioactive substances, including beta-glucans, phenolic compounds, B vitamins, and, most importantly, the high concentration of polyunsaturated fatty acids, such linoleic acid, are beneficial for human health advantages [16].

Mushroom bioactive compounds have anti-cancerous activity because they include glucans, sesquiterpenes, glycoproteins, or peptide/protein-bound polysaccharides, mushrooms have been shown to have antitumor effects mostly through immune system modulation [17][18].

Additionally, mushrooms include a number of vitamins (such as thiamin, riboflavin, ascorbic acid, and vitamin D), minerals, amino acids, and other chemical substances that all contribute to their overall health advantages [18].

Certain natural mushroom chemicals have been shown to negatively affect particular molecular targets involved in angiogenesis, cell survival, and proliferation, as well as to exhibit specific efficacy against signalling pathways that are abnormally activated in cancer cells [19] [20]. Both preclinical and clinical studies have been conducted to examine the possible therapeutic benefits of mushrooms. In recent years, a number of high-quality evaluations have compiled the effects of mushrooms and mushroom extracts on human illness, particularly cancer [21] [22].

The present study aims to systematically evaluate the *in-vitro* anticancer potential of medicinal and edible mushrooms, with a specific focus on *P. sajor-caju*, in the context of breast cancer. This investigation encompasses both direct and indirect mechanisms underlying their anti-tumoral activity. Comprehensive literature mining was conducted to identify and analyze experimental studies, meta-analyses, and clinical findings related to mushroom-derived compounds and their modulatory effects on breast cancer cell lines and patient outcomes. In particular, the study explores bioactive constituents from *P. sajor-caju*, elucidating their potential molecular pathways—including apoptosis induction, immune modulation, and inhibition of cell proliferation—that contribute to breast cancer suppression. Despite extensive research into cancer treatment, traditional methods such as chemotherapy, radiation, and surgery have only slightly improved tumour prognoses [23]. Furthermore, data on dietary mushroom intake and its epidemiological correlation with reduced breast cancer risk were systematically reviewed, providing an integrative perspective on both therapeutic and preventive roles of medicinal and edible mushrooms in breast cancer management [22].

## 2. Materials and methods

## 2.1 Collection and screening of potential bioactive compounds *P. sajor – caju* mushroom

Behalf of most recent literature, [24] [25] bioactive compounds identified from *P. sajor-caju* with reported or potential anticancer properties were systematically retrieved. Their three-dimensional (3D) molecular structures and chemical characteristics were obtained from the PubChem database (https://pubchem.ncbi.nlm.nih.gov/). The standard "Simplified Molecular Input Line Entry System (SMILES)" for all chemical 3D Conformations and strings were gathered for additional computer analysis [26].

Subsequent *in-silico* screening was performed to assess the drug-likeness and oral bioavailability of the retrieved compounds. Molecular descriptors were evaluated according to Lipinski's Rule of 5, a widely accepted guideline for drug-like properties [11]. Compounds satisfying the following criteria were considered suitable for further analysis: molecular weight ≤ 500 Da, LogP ≤ 5, hydrogen bond donors (HBD) ≤ 5, and hydrogen bond acceptors (HBA) ≤ 10[27]. For molecular docking and further virtual screening, only compounds that satisfied these criteria were shortlisted.

## 2.2 Prioritization of target proteins

The breast cancer-related gene data (DOID:1612, Homo sapiens) were retrieved from the STRING database (https://string-db.org/), further, utilized a high-confidence interaction score threshold to ensure network reliability. The resulting protein–protein interaction (PPI) network was exported and visualized using Cytoscape platform—a widely used standalone bioinformatics platform for network analysis [28]. Hub gene prioritization was conducted using the CytoHubba plugin within Cytoscape, employing multiple topological algorithms, including Radiality, Closeness, Edge Percolated Component (EPC), Maximum Neighbourhood Component (MNC), Degree, and Maximal Clique Centrality (MCC), to ensure comprehensive hub gene identification [29]. The "Research Collaboratory for Structural Bioinformatics Protein Data Bank" (RCSB PDB; https://www.rcsb.org/) provided the 3D structures of the top-ranked hub proteins. The selection of PDB entries was based on stringent structural quality criteria, including a resolution better than 2.5 Å, experimental method preference in the order: X-ray crystallography > cryo-electron microscopy (cryo-EM) > nuclear magnetic resonance (NMR), and completeness of the target chain with minimal missing residues, particularly within the active or binding site regions. Selected protein structures were downloaded in .pdb format for downstream molecular docking and interaction analysis.

## 2.3 Molecular docking simulation study

## 2.3.1 Preparation of target protein

The 3D structures of the prioritized hub proteins were prepared for molecular docking following the protocol described by [28]. using BIOVIA Discovery Studio 2021. Initially, crystallographic water molecules and all non-essential heteroatoms (such as ligands, ions, and co-crystallized compounds) were removed from the targeted protein, retaining only the desired chain. Polar hydrogen atoms were subsequently added to facilitate hydrogen bond recognition, and Gasteiger and Coulomb charges were computed to model electrostatic interactions effectively [30].

The processed protein structures were saved in .pdb format as protein.pdb in the working directory. For docking studies, the target proteins were further prepared as rigid receptors using Auto Dock Vina integrated within PyRx software. After assigning torsion constraints and receptor definitions, the final receptor files were saved in. pdbqt format (protein. pdbqt) for use in virtual screening and molecular docking simulations.

## 2.3.2 Preparation of ligand molecules

Initially, the potential oral active drugs' 3D structures were obtained in the Sapital Data File (SDF) format and opened through PyMOL for structural visualization. Each compound was converted from SDF to PDB format to ensure compatibility with downstream docking protocols through Open babel tool. Subsequently, the PDB files were imported into the AutoDock Tools (ADT) platform for ligand preparation. During this process, torsional bonds were defined, non-polar hydrogens were merged, and Gasteiger charges were assigned to facilitate accurate molecular docking. Finally, all ligands were saved in the AutoDock compatible pdbqt format (e.g., ligand. pdbqt) and prepared for docking against the target proteins using AutoDock Vina.

## 2.3.3 Grid preparation

The grid preparation is a critical step that defines the search space for ligand-receptor interactions [31]. Using AutoDock Vina, the receptor protein was first converted to PDBQT format and loaded into the docking workspace. Ligand molecules, also in PDBQT format, were selected, and a configuration file (confi.txt) was generated specifying grid size, exhaustiveness, and the three-dimensional coordinates (X, Y, Z) of the binding site. These parameters guided the docking simulations by accurately delimiting the binding region.

## 2.3.4 Run the docking program

The first molecular docking study was conducted through PyRx (an open-source virtual screening platform) for the screening potentially interacted orally active compounds against the prioritized targets. Prepared receptor chains were loaded as targets, and a library of ligands was imported and energy-minimized of all ligands. Docking was performed with default Vina parameters, and binding affinities (in kcal/mol) were calculated for each ligand pose.

## 2.3.5 Confirmatory molecular docking

The again docking experiment was performed by AutoDock Vina (an open-source tool) widely used for confirmation of predicted binding affinities by PyRx and optimal ligand poses with target proteins [32]. This tool used a gradient-based conformational search and executed the binding affinity using the command **vina.exe –config conf.txt –log log.txt**, enabling evaluation of interactions between rigid receptors and flexible ligands. For the split docked poses, the **vina_split.exe –input out.pdbqt** command was employed. The docking protocol followed a previously established methodology [31], ensuring robustness and consistency in pose orientation and binding affinity estimation.

## 2.4 Root mean square fluctuations (RMSFs) analysis

The RMSF used to investigate the protein's flexible states in the receptor-ligand docked complex, which are functionally significant to validation of molecular docking study [28]. The "CABS-flex 2.0 server (https://biocomp.chem.uw.edu.pl/CABSflex/about.php)" was used to analyze the best-docked poses using its default settings. A temperature of 1.4 affects flexibility, and it has 10 ns simulation cycles for balanced accuracy and efficiency. The 10 typical models for structural analysis make up the final ensemble, which is formed by clustering using a 3.0 threshold and force field weights of 1.0 for CA-CA distance constraints and secondary structure [28].

## 2.5 Cell line study

A publicly accessible web-service called "PASS CLC Pred (https://www.way2drug.com/Cell-line/)" was utilized to addressed the cytotoxicity of possible drugs against breast cancer cell lines. The quantitative structure activity relationship (QSAR), connection mapping, network pharmacology, and machine learning algorithms are inbuilt in the tool among the essential techniques to establishment of cell line study [28]. used in contemporary drug development. While connection mapping compares drug-induced gene expression profiles to find possible targets, QSAR associates chemical structures with cytotoxicity. Pharmacology in networks provides insights into therapeutic mechanisms by exposing intricate biological relationships [33].

## 2.6 ADMET Profile of potent lead compound

In drug discovery protocols, the Absorptions, Distributions, Metabolism, Excretion and Toxicity (ADMET) characteristics are essential for evaluating their pharmacokinetic and pharmacodynamic profiles [11]. The Swiss ADME (https://www.swissadme.ch/) and pkCSM (https://biosig.lab.uq.edu) were used to determination of ADMET properties of anticancer lead compounds of mushroom.

# 3. Results and discussion

## 3.1 A bioactive compounds of *P. sajor – caju* mushroom

In the current study total 22 bioactive compounds of mushrooms were taken, including Ethyl iso-allocholate, Benzyl butyl phthalate, 1-((1-butoxypropan-2-yl)oxy)propan-2-ol, Phenylacetaldehyde, 3-Trifluoroacetoxytetradecane, Caryophyllene, Acetic acid, 2,4-di-tert-butylphenol, 3-Chloropropionic acid 3-pentadecyl ester, 1,2-benzenedicarboxylic acid bis(2-methylpropyl) ester, 2,3-dimethyl-5-(trifluoromethyl)benzene-1,4-diol, Hexadecanoic acid, Linoleic acid, 1-Monolinolenoyl-rac-glycerol, Isoeugenol, 9,12-Octadecadienoicacid, Eicosanoic acid, 10,12-Docosadiynedioic acid, Linalool. For the comparative study, 2 standard anticancer drugs such as Capecitabine and Veliparib, previously reported to be derived from mushrooms, were included as positive controls based on studies by [24][25].

The molecular descriptors of these selected compounds, offering detailed insights into their structural features, chemical characteristics, and physicochemical properties relevant to their biological activity has been given in Table 1.

Table 1
Key molecular descriptors of selected bioactive compounds of *P. sajor caju* and their oral activity status *by used of* Lipinski's Rule of Five (RO5).

| Sr. No. | Bioactive compound name | PubChem ID | Molecular formula | Molecular weight (g/mol) | H-bond donar | H-bond acceptor | LogP value | Oral activity status |
|---|---|---|---|---|---|---|---|---|
| **1.** | **Ethyl iso-allocholate** | **6452096** | **C26H44O5** | **436.6** | **3** | **5** | **4.3** | **Yes** |
| 2. | Benzyl butyl phthalate | 2347 | C19H2004 | 312.4 | 0 | 4 | 4.9 | Yes |
| 3. | 1-((1-Butoxypropan-2-yl) oxy) propan-2-ol | 242752 | C17H1204 | 160.17 | 2 | 4 | 1.2 | Yes |
| 4. | Phenylacetaldehyde | 998 | C8H8O | 120.15 | 0 | 1 | 1.8 | Yes |
| 5. | 3-Trifluoroacetoxytetradecane | 534404 | C16H2F3O2 | 310.39 | 0 | 5 | 7.8 | No |
| 6. | Caryophyllene | 5281515 | C15H24 | 204.35 | 0 | 0 | 4.4 | Yes |
| 7. | Acetic acid | 5282110 | C11H1202 | 176.21 | 1 | 2 | 2.3 | Yes |
| 8. | 2,4-Di-tert-butylphenol | 7311 | C14H220 | 206.32 | 1 | 1 | 4.9 | Yes |
| 9. | 3-Chloropropionic acid, 3-pentadecyl ester | 561103 | C18H35ClO2 | 318.9 | 0 | 2 | 7.7 | No |
| 10. | 1,2-Benzenedicarboxylic acid bis(2-methylpropyl)ester | 6782 | C16H22O4 | 278.34 | 0 | 4 | 4.1 | Yes |
| 11. | 2,3-Dimethyl-5-(trifluoromethyl) benzene-1,4-diol | 590850 | C9H9F3O2 | 206.16 | 2 | 5 | 2.2 | Yes |
| 12. | Hexadecanoic acid | 985 | C16H32O2 | 256.42 | 1 | 2 | 6.4 | No |
| 13. | Linoleic acid | 5280450 | C18H32O2 | 280.4 | 1 | 2 | 6.8 | No |
| 14. | 1-Monolinolenoyl-rac-glycerol | 5367328 | C21H36O4 | 352.5 | 2 | 4 | 5.1 | No |
| 15. | Isoeugenol | 853433 | C10H12O2 | 164.20 | 1 | 2 | 2.6 | Yes |
| 16. | Tetraacetyl-d-xylonic nitrile | 541568 | C14H17NO9 | 343.29 | 0 | 10 | -0.4 | Yes |
| 17. | 9,12-Octadecadienoicacid | 60107946 | C66H125NO5 | 1012.7 | 3 | 5 | 26.2 | No |
| 18. | Eicosanoic acid | 537899 | C29H62O4Si2 | 531.0 | 0 | 4 | - | No |
| 19. | 10,12 –Docosadiynedioic acid | 544138 | C22H34O4 | 362.5 | 2 | 4 | 6.7 | No |
| 20. | Linalool | 6549 | C10H18O | 154.25 | 1 | 1 | 2.7 | Yes |
| 21. | Capecitebine | 60953 | C15H22FN3O6 | 359.35 | 3 | 7 | 0.6 | Yes |
| 22. | Valiparib | 11960529 | C13H16N4O | 244.29 | 3 | 3 | .5 | Yes |

## 3.2 Oral activity status of bioactive candidates of *P. sajor – caju*

In this study, the Lipinski's Rule of Five is a widely accepted theoretical guideline used to differentiated orally active lead candidates from taken bioactive compounds of mushroom. Out of the 22 bioactive compounds, 14 compounds viz. Ethyl iso-allocholate, Benzyl butyl phthalate, 1-((1-butoxypropan-2-yl)oxy)propan-2-ol, Phenylacetaldehyde, Caryophyllene, Acetic acid, 2,4-di-tert-butylphenol, 1,2-benzenedicarboxylic acid bis(2-methylpropyl) ester, 2,3-dimethyl-5-(trifluoromethyl)benzene-1,4-diol, Isoeugenol, Tetraacetyl-d-xylonic nitrile and Linalool with anticancerous drug Capecitebine, Valiparib were found to comply with Lipinski's criteria and were thus classified as potentially orally active. The rest bioactive compounds such as Eicosanoic acid, 9,12-Octadecadienoic acid, 10,12-Docosadiynedioic acid, Hexadecanoic acid, Linoleic acid, 1-Monolinolenoyl-rac-glycerol, 3-Chloropropionic acid 3-pentadecyl ester and 3-Trifluoroacetoxytetradecane did not meet Lipinski's parameters and were therefore categorized as non-orally active compounds.

## 3.3 Protein-protein interaction (PPI) network analysis and prioritization of Hub genes for breast cancer

The PPI network for putative breast cancer developing proteins was built using machine learning methods and sophisticated graph theory in the STRING database. 22 proteins were found in a network with 62 nodes, 507 edges, and an average node degree of 16.4 in this PPI network (Fig. 1 [A]) investigation. A considerable degree of connection between the proteins was shown by the average local clustering coefficient, which was determined to be 0.672. The observed number of edges was substantially greater than the expected amount (191), indicating robust network enrichment. The p-value for PPI enrichment was discovered to be less than 1.0e-16, indicating that the network's interactions were biologically relevant rather than random.

MCC measures the relationship between expected and actual classifications while ordering proteins, efficiently balancing "true positives (TP), true negatives (TN), false negatives (FN) as well as positives (FP). The hub proteins with the highest MCC scores in the current 10 hub protein network are CDKN2A and 1D5R, which are important for the network's operation and regulatory significance (shown in Fig. 1[B] as dark orange). Other proteins with high rankings, like CDH1, EGFR, and EGF, also showed strong centrality (seen in Fig. 1 [B] as pale orange and yellow). The proteins MYC and ESR1 are also important in the development of breast cancer (seen in Fig. 1[B] as a faint red colour). This PPI's peripheral or specialised functions were indicated by the helpful but moderately interacting proteins ERBB2, BRCA1, TP53, and ESR1 (shown in red in Fig. 1 [B]). A Cytoscape plugin called CytoHubba was utilised to rank the hub proteins in the current PPI and determine the "Matthews Correlation Coefficient (MCC)" (Fig. 1 [C]).

In totality, 10 proteins including CDKN2A, ERBB2, BRCA1, TP53, ESR, CDH1, EGF, PTEN, EGFR, ESR1 and MYC” were found as significant associated to each other in relation to breast cancer propagation in humans.

## 3.4 Structural analysis and binding site prediction of hub proteins

The 3D structure of 10 proteins such as TP53-binding protein-1 (TP53), Phosphoinositide phosphatase PTEN (PTEN), anti-EGFR antibody FV region (EGFR), C-Myc-binding protein (MYC), protein MEMO1 (ERBB2), BRCA1-associated RING domain protein-1 (BRCA1), Jagged-2 signaling protein (EGF), chromodomain-helicase-DNA-binding protein-1 (CDH1), Estrogen receptor (ESR1) and arginine N-methyltransferase-5 (CDKN2A) were retrieved from RCSB PDB database from their PDB IDs such as 8SWJ, 1D5R, 1WT5, 2YYO, 3BCZ, 3FA2, 5MWF, 4B4C, 6PSJ and 5FA5 respectively shown in supplementary table 1.

The potential ligand-binding sites across the 10 selected target proteins was predicted by an online PrankWeb server. The study revealed that TP53-binding protein-1 exhibited the highest binding score (44.2) with a strong binding probability of (0.968), indicating a highly confident prediction. In similar way the protein MEMO1 also showed high score of (29.22) with a probability of (0.913), supporting its potential as a strong binding target. Some other hub proteins like arginine N-methyltransferase 5 (score: 8.95; probability: 0.526) and the anti-EGFR antibody FV region (score: 6.86; probability: 0.385) showed moderate binding confidence. The breast cancer hub proteins such as chromodomain-helicase-DNA-binding protein 1 (score: 0.89; probability: 0.005) and C-Myc-binding protein (score: 2.94; probability: 0.096) demonstrated low predicted binding site probabilities, suggesting limited confidence in ligand binding at the predicted site. In Table 2 the detailed scores, probabilities, and binding residues of each protein has been given.

Table 2
Residues wise binding site prediction of target protein based on the probability and binding score through Prank Web 2.0 server.

| Target Protein | Score | Probability | Pocket Centre (X, Y, and Z axis) | Binding residues |
|---|---|---|---|---|
| TP53-binding protein-1 | 44.2 | 0.968 | 27.9228, -1.6166, and 29.5261 | 1495, 1497, 1498, 1500, 1502, 1503, 1519, 1521, 1523, 1545, 1547, 1548, 1550, 1551, 1553, 1584, 1587, 1495, 1497, 1498, 1500, 1502, 1503, 1519, 1520, 1521, 1523, 1547, 1548, 1552, 1553, 1584, and 1587 |
| Phosphoinositide phosphatase PTEN | 5.08 | 0.242 | 34.5429, 87.4174, and 25.7949 | 124, 125, 126, 128, 129, 130, 167, 168, 171, 92, and 93 |
| Anti-EGFR antibody FV region | 6.86 | 0.385 | 19.5538, 30.6106, and 0.8291 | 110, 111, 112, 113, 8, 9, 93, 110, 111, 113, 39, 93, 46, 108, 43, 45, 46, 47, and 90 |
| C-Myc-binding protein | 2.94 | 0.096 | 22.3314, 13.6673, and 10.5983 | 151, 53, 55, 70, 73, 81, 83, 84, 88, and 92 |
| Protein MEMO-1 | 29.22 | 0.913 | -28.3530, -16.8120, and − 33.6480 | 12, 129, 131, 15, 158, 159, 16, 160, 189, 192, 197, 242, 244, 246, 247, 287, 289, 49, 50, 51, 54, 79, 80, 81, and 82 |
| BRCA1-associated RING domain protein-1 | 4.6 | 0.212 | 15.0175, 17.4590, and − 43.8095 | 567, 570, 604, 605, 606, 627, 628, 629, 648, 661, 664, and 665 |
| Jagged-2 signaling protein | 4.93 | 0.232 | 35.8494, 33.3914, and − 30.5640 | 132, 133, 134, 135, 136, 88, 90, 91, 92, 133, 72, 86, 88, 89, 90, 91, and 92 |
| Chromodomain-helicase-DNA-binding protein 1 | 0.89 | 0.005 | 19.9307, -3.7593, and 24.0345 | 1140, 1141, 1142, 1143, 1147, 1221, 1224, 1225, 1265, and 1266 |
| Protein arginine N-methyltransferase 5 | 8.95 | 0.526 | -18.9903, -100.7936, and − 4.7222 | 314, 315, 319, 324, 327, 365, 367, 370, 392, 393, 419, 420, 435, 436, 444, and 449 |
| Estrogen receptor (ESR1) | 31.94 | 0.927 | 23.8594, -41.6573, and 18.8978 | 343, 346, 347, 349, 350, 351, 353, 354, 383, 384, 387, 388, 391, 394, 404, 421, 424, 425, 428, 421, 522, 524, 525, 526, 536, and 539 |

# 3.5 Molecular docking study

The present molecular docking study evaluated the binding affinities of selected bioactive compounds and elucidated the interaction patterns within potential receptor–ligand complexes. A total of 12 bioactive compounds, along with 2 standard anticancer drugs, were employed as ligands against the prioritized 10 hub proteins associated with breast cancer development. The protein-wise molecular docking results are summarized below and the binding affinity graph has depicted in Fig. 2 and tabulated in Supplementary Table 2

**3.5.1 Arginine N-methyltransferase-5**: Out of 14 potent orally active compounds, 5 potential inhibitors exhibited strong interactions with Benzyl butyl phthalate (− 8.5 kcal/mol), Ethyl iso-allocholate (− 7.8 kcal/mol), Caryophyllene (− 7.7 kcal/mol), 1,2-Benzenedicarboxylic acid bis(2-methylpropyl) ester (− 7.3 kcal/mol), and Acetic acid (− 7.6 kcal/mol) against the protein arginine N-methyltransferase-5. The minimum binding affinity exhibited the strong interaction between the receptor-ligand docked complexes [11]. While the observed binding affinities of standard drugs such as Veleparib (− 7.1 kcal/mol) and Capecitebine (− 6.6 kcal/mol) were comparatively weak against the selected target proteins. In present comparative docking analysis against the target protein arginine N-methyltransferase-5, the compound Benzyl butyl phthalate exhibited a potent complex with the target protein CDKN2A, further supporting it as a potent anticancer bioactive compound of mushroom. [34] reported that the derivatives phthalate has potent antiproliferative activity and they exhibit anti-inflammatory and anticancer potential.

**3.5.2 TP53-binding protein-1**: The TP53-binding protein-1, a crucial mediator in the p53 tumor suppressor pathway that is malignancy of humans [35]. The present molecular docking study identified 3 promising inhibitors with the lowest binding affinity such as Caryophyllene (-7.8 kcal/mol), Ethyl iso-allocholate (-7.4 kcal/mol), and Benzyl butyl phthalate (-7.2 kcal/mol), The other bioactive compounds were obtained potential binding affinity such as 1,2-benzenedicarboxylic acid bis(2-methylpropyl)ester (-6.5 kcal/mol), Acetic acid (-6 kcal/mol), Phenylacetaldehyde (-5.9 kcal/mol), 1-((1-butoxypropan-2-yl)oxy)propan-2-ol (-4.1 kcal/mol), and they were also similar range of binding affinity of standard drugs such as Veleparib (-6.4 kcal/mol), Capecitebine (-6.3 kcal/mol) against the same target protein. The present comparative study observed that the binding affinity of all OACs were good than selected anticancer compound that Caryophyllene binds effectively to the active site of *Homo sapiens* with a binding energy of (-7.8 kcal/mol). Natural bicyclic sesquiterpenes, β-caryophyllene (BCP) and its oxidized form β-caryophyllene oxide (BCPO), are widely distributed in various plant species. Both compounds exhibit notable anticancer properties by inhibiting the growth and proliferation of diverse cancer cell types 36.

**3.5.3 Protein MEMO-1**: The protein MEMO-1, a key mediator of peptide binding, is associated with human malignancies [37]. The present molecular docking study, 5 promising leads were identified with the strong binding affinity among the screened OACs such as Ethyl iso-allocholate (− 7.9 kcal/mol), 2,3-dimethyl-5-(trifluoromethyl) benzene-1,4-diol (− 7.7 kcal/mol), 1,2-benzenedicarboxylic acid bis(2-methylpropyl) ester (− 6.6 kcal/mol), Acetic acid, (− 6.4 kcal/mol), and Caryophyllene (− 6.3 kcal/mol). The Ethyl iso-allocholate exhibited the highest binding affinity (− 7.9 kcal/mol), indicating strong potential as an inhibitor of MEMO1 compared to binding affinity of taken standard drugs; Veleparib (-7.3 kcal/mol) and Capecitebine (-7.6 kcal/mol).

**3.5.4 Phosphoinositide phosphatase (PTEN)**: The PTEN tumor suppressor protein, a critical hydrolase involved in the regulation of cell growth and malignanc[38], was targeted in the present molecular docking study. Out of 14 potent OACs, 4 compounds such as Ethyl iso-allocholate (− 7.8 kcal/mol), Benzyl butyl phthalate (− 7.7 kcal/mol), Caryophyllene (− 6.8 kcal/mol), and Acetic acid (− 6.2 kcal/mol) predicted promising lead against the PTEN. The compound Ethyl iso-allocholate demonstrated the highest binding affinity, suggesting its potential as a strong PTEN inhibitor in compare to anticancer drugs like Veleparib (-7.1 kcal/mol), Capecitebine (-7.6 kcal/mol). From the interpretation Ethyl iso-allocholate against PTEN, show anticancer activity of further supporting its potential as an effective candidate for cancer therapy targeting tumor suppressor pathways [38].

**3.5.5 BRCA-1-associated RING domain protein-1**: The BRCA-1-associated RING domain protein-1, a peptide-binding protein critically involved in tumorigenesis [39] was identified as hub therapeutic target in the present comparative molecular docking study. The 5 promising lead candidates, 2,3-dimethyl-5-(trifluoromethyl) benzene-1,4-diol (− 6.8 kcal/mol), Ethyl iso-allocholate (− 6.5 kcal/mol), 2,4-di-tert-butylphenol (− 6.1 kcal/mol), Caryophyllene (− 6.1 kcal/mol), and Benzyl butyl phthalate (− 5.8 kcal/mol) were potent binding affinity against BRCA1. In compare to standards drugs Veleparib (-6.7 kcal/mol), Capecitebine (-6.6 kcal/mol) these 5 candidates were also similar range of binding affinity.

**3.5.6 C-Myc-binding protein**: Hub target C-Myc-binding protein, a key peptide-binding protein implicated in human malignancies [39]. Present docking study identified 6 promising OACs with notable binding affinities: Ethyl iso-allocholate (− 6.7 kcal/mol), Caryophyllene (− 5.2 kcal/mol), 2,3-dimethyl-5-(trifluoromethyl) benzene-1,4-diol (− 5.8 kcal/mol), Acetic acid (− 5.5 kcal/mol), Benzyl butyl phthalate (− 5.4 kcal/mol), and 2,4-di-tert-butylphenol (− 5.3 kcal/mol). The Ethyl iso-allocholate demonstrated the highest binding affinity among the other prominent leads, suggesting its potential as a promising inhibitor of the Myc-binding protein involved in cancer progression. The study of [40] reported that in most of the anticancer plant remedies has major phytoconstituents (Ethyl iso-allocholate).

**3.5.7 Protein CDH-1**: Above prioritized hub target DNA-binding domain of the human protein CDH-1, a critical regulator of gene expression and cell adhesion associated with malignancy [41] was explored as a therapeutic target present docking study. The 5 potent OACs viz. Ethyl iso-allocholate (− 6.6 kcal/mol), Benzyl butyl phthalate (− 5.9 kcal/mol), 2,3-dimethyl-5 (trifluoromethyl)benzene-1,4-diol (− 5.8 kcal/mol), 1,2-benzenedicarboxylic acid bis(2-methylpropyl) ester (− 5.7 kcal/mol), and Caryophyllene (− 5.6 kcal/mol) of selected mushroom exhibited a good binding affinity against CDH-1. The Ethyl iso-allocholate comparable binding affinity with the standards Veleparib (-6.6 kcal/mol), Capecitebine (-6.2 kcal/mol). The present study advocated that the phyto-compound (Ethyl iso-allocholate) of mushroom has a good potency for targeting the DNA-binding domain of CDH1 in cancer therapeutics [42][40].

**3.5.8 Epidermal growth factor receptor (EGFR)**: The EGFR protein is significant mediator in the human immune response and cell signaling [43]. Out of 14 potent OACs, 5 compounds exhibited notable binding affinities against EGFR: Benzyl butyl phthalate (− 6.1 kcal/mol), Ethyl iso-allocholate (− 6.0 kcal/mol), Caryophyllene (− 5.7 kcal/mol), Acetic acid (− 5.3 kcal/mol), and 1,2-benzenedicarboxylic acid bis(2-methylpropyl) ester (− 5.2 kcal/mol). The compounds such as Benzyl butyl phthalate and Ethyl iso-

allocholate demonstrated the strongest binding interactions and they have potent docked configuration in similar to standard drugs Veleparib (-5.4 kcal/mol), Capecitebine (-5.8 kcal/mol).

**3.5.9 Epidermal growth factor (EGF)**: Out of 10 hub proteins the EGF protein, a key signaling molecule involved in cell growth, proliferation, and differentiation in humans [44]. The 5 potential leads demonstrated favorable binding affinities: Ethyl iso-allocholate (− 7.4 kcal/mol), 2,3-dimethyl-5-(trifluoromethyl) benzene-1,4-diol (− 6.1 and − 6.0 kcal/mol), Caryophyllene (− 5.7 kcal/mol), and Benzyl butyl phthalate (− 5.4 kcal/mol) against the epidermal growth factor (EGF) protein. The Ethyl iso-allocholate exhibited the similar binding affinity to taken similar standards viz. Veleparib (-6.4 kcal/mol), Capecitebine (-6.6 kcal/mol).

**3.5.10 Estrogen receptor (ESR1)**: The ESR1 protein is significant mediator in the human immune response and cell signaling [45]. Out of 14 potent OACs, 5 compounds exhibited notable binding affinities against EGFR: Benzyl butyl phthalate (− 6.9 kcal/mol), Ethyl iso-allocholate (− 7.0 kcal/mol), Caryophyllene (− 6.5 kcal/mol), 2,4-di-tert-butylphenol (− 6.4 kcal/mol), and 1,2-benzenedicarboxylic acid bis(2-methylpropyl) ester (− 6.1 kcal/mol). The compounds such as Benzyl butyl phthalate and Ethyl iso-allocholate demonstrated the strongest binding interactions and they have potent docked configuration in similar to standard drugs Veleparib (-8.4 kcal/mol), Capecitebine (-7.4 kcal/mol).

The 2 potential OACs such as Ethyl iso-allocholate and Benzyl butyl phthalate were predicted as the most promising OACs of *P. sajor-caju* with consistent and significant binding affinities across all prioritized hub proteins associated with breast cancer. These compounds demonstrated binding energies comparable to, or in some cases exceeding, those of standard anticancer agents, suggesting their strong potential as lead candidates for targeted cancer therapy. Notably, Ethyl iso-allocholate has been previously reported for its antiproliferative and anti-inflammatory properties, supporting its therapeutic relevance in cancer models [40][46]. [47] reported that the compound Benzyl butyl phthalate has shown cytotoxic effects in various cancer cell lines, particularly through mechanisms involving oxidative stress and apoptosis. The consistency of binding interactions with key oncogenic targets such as PTEN, BRCA1, CDH1, EGFR, and MYC further supports their potential as multitarget inhibitors. A recent published study by [48] also suggested both compounds have prominent anti oncogenic activity. With the present findings both compounds suggested further validation through *in-vitro* assays, *in-vivo* studies, and ultimately clinical trials to assess their efficacy, bioavailability, and safety profiles in cancer therapeutics.

# 3.6 Receptor-ligand Interaction pattern analysis of potential docked pose

The present study revealed that mushroom-derived prominent compounds; Ethyl iso-allocholate and Benzyl butyl phthalate interacted with hub protein MEMO-1 and arginine N-methyltransferase-5 through various functional groups, forming stable bindings via hydrogen bonds, π-π stacking, van der Waals forces, π-alkyl, and other interactions, indicating strong binding affinities. The study reported that the protein arginine N-methyltransferase-5 interacted with Ethyl iso-allocholate, through the 3 active residues: HIS507, PHE509 and ASN508 by Conventional Hydrogen bonding with bond lengths of 2.34 Å, 1.93 Å, 2.40 Å, and 2.58 Å, respectively. The van der Waals interactions were also found with specific amino acids such as GLU298, TYR297, GLU306, HIS510, GLN511, LEU222, GLY223 and LEU506 of receptor chain. The active residues: ARG256, LEU260 and LYS259 interacted through an Alkyl and Pi-Alkyl bond with a bond length of 5.10 Å, 4.92 Å, 5.19 Å and ARG506 by Carbon Hydrogen Bond of the same docked pose shown in Fig. 3 [A].

Similarly, the protein arginine N-methyltransferase-5 interacted with the Benzyl butyl phthalate through the receptor residue PHE580, by conventional hydrogen bond with a bond length of 2.13 Å. The hydrogen bonds play a crucial role in molecular docking by stabilizing ligand–receptor complexes, enhancing binding specificity and orientation of ligand binding at the active site [11]. Along with this bonding, the van der Waals associations were acquired using the active residues as well receptor chains viz. GLU435, LEU437, SER439, LYS333, PRO311, SER310, GLN309 and SER578. Some other residues such as LEU312, PHE327 were interacted with Benzyl butyl phthalate through a Pi-alkyl, alkyl, Pi-Pi Stacked bond with a bond length of 4.45 Å, 4.66 Å and 3.84 Å respectively. In the continuation of binding pattern analysis some important bond like Pi-Sigma which attached to ligand with VAL503 residue with bond length of 3.60 Å, Carbon Hydrogen Bond also attached with TRP579 (3.41 Å), GLU444 (3.29 Å), PHE300, VAL326 residues shown in Fig. 3 [B].

The protein MEMO-1 interacted to Ethyl iso-allocholate via receptor residues ARG246, THR242, PHE197, SER286, SER277, TYR277, TYR289, TRP16, HIS49 and ASP189 by van der Waals forces. The 2 residues such as HIS192 and SER276 interacted with Conventional Hydrogen Bond, with a bond length of 2.37 Å, and 2.37 Å respectively. Additionally, CYS244, HIS81, HIS131, ALA50, TYR54, and VAL287 interacts through both Pi-Alkyl and Alkyl Stacked, with bond lengths of 4.41 Å, 4.40Å, 4.39 Å, 5.13 Å, 5.19 Å, 5.11 Å, and 4.89 Å (Fig. 4 [A]).

The active residues SER222, ASP217, GLY220, TYR273, GLU225, ASN272 and LEU271 were interacted via van der Waals interactions in the docked pose of MEMO-1 and Benzyl butyl phthalate. The residue ALA290 interacted with the bond length of a Pi-alkyl bond is

4.50 Å. One residue LYS218 interacted via Conventional Hydrogen Bond with the bond length of 2.67 Å in the same docked pose for their potential stability [27]. The two residues PHE190 and PHE270 were mapped with ligand through Pi-Pi Stacked and Pi-Pi-shaped with bond lengths of 5.70Å and 4.00 Å (Fig. 4 [B]).

# 3.7 Docked pose stability analysis by RMSF

The root means square fluctuations (RMSF) check the flexibility of protein residues during molecular dynamics simulations and it also highlighting binding sites with significant conformational changes [28]. The present fluctuation plot of protein arginine N-methyltransferase-5 illustrates the residue-wise atomic fluctuations of the protein backbone in complex with Ethyl iso-allocholate (blue) and Benzyl butyl phthalate (orange) (Fig. 5 [A]). Ethyl iso-allocholate and Benzyl butyl phthalate exhibited similar fluctuation pattern showcase the comparable dynamic behaviour of the protein-ligand complexes throughout the simulation. There were several distinct regions showed differential flexibility in the docked complexes of Ethyl iso-allocholate and Benzyl butyl phthalate with the receptor protein (arginine N-methyltransferase-5). The active residues around positions 1–25, 65–75, 109–115, 133–139, and 253–271 demonstrated higher RMSF values, indicating localized flexibility [28]. In case of Benzyl butyl phthalate binding resulted in slightly elevated fluctuations at multiple active sites such as 65–75 and 133–139, suggesting a greater degree of local motion compared to Ethyl iso-allocholate [28]. However, Ethyl iso-allocholate showed a sharp spike in flexibility at residues 265–270, surpassing that of Benzyl butyl phthalate, which could indicate a region-specific destabilization or structural rearrangement [28]. The active residues of receptor protein remained largely stable during simulation, with RMSF values for most residues falling below 2.0 Å, except for loop and terminal regions which are inherently more flexible. These findings suggest that both ligands interact stably with the protein and supposed to distinct local dynamic influences [28].

The molecular dynamics simulation of MEMO-1 protein upon binding with Ethyl iso-allocholate (blue) and Benzyl butyl phthalate (orange) showcasing the fluctuation patterns in Fig. 5 [B]. These potential inhibitors showed a notable difference in specific regions of the active sites of receptor chain pattern. A significant pick was observed for the Ethyl iso-allocholate complex around residues 40–60, where the fluctuations values reach a maximum of nearly 8 Å, suggesting significant flexibility or possible loop motion in this region. In the docked complex of Benzyl butyl phthalate induces comparatively lower fluctuations at the same region, indicating a stabilizing [11]. Moreover, differential peaks were observed at residues position 150–160, 330–340, 480–500, and 540–560, where either ligand induces localized mobility. Notably, Benzyl butyl phthalate shows sharp spikes around residues 330 and 340, surpassing Ethyl iso-allocholate, suggesting enhanced dynamic behavior in these segments [28].

In present RMSF analysis most residues-maintained fluctuation values below 3 Å and found that both complexes were stable over the period of dynamics simulations. The terminal residues and loop residues exhibited higher fluctuations, However, the core residues remained relatively stable. This simulation study revealed that both ligands were stable docked poses with the receptor protein. The Ethyl iso-allocholate induces a higher degree of fluctuation in terminal regions whereas Benzyl butyl phthalate shows more fluctuation in the mid active residues and later regions.

# 3.9 Comparative cell line study

The cytotoxic potential of predicted lead compounds was assessed using the CLC-Pred web server, which predicts compound activity against breast cancer cell lines based on structural formulae. The lead compounds Benzyl butyl phthalate and Ethyl iso-allocholate showed notable probabilities of activity (Pa values) at 0.321 and 0.320, respectively, with corresponding probabilities of inactivity (Pi values) at 0.044 and 0.267. Both the compounds demonstrated Pa values exceeding 0.3 and higher than their respective Pi values, suggesting a promising cytotoxic potential and supporting the molecular docking outcomes observed in this study [28].

The present cell line study found that the standard anticancer drugs, Capecitabine and Valiparib exhibited lower Pa values of 0.251 and 0.197, respectively, with Pi values of 0.063 for Capecitabine and 0.197 for Valiparib. While Capecitabine still showed a higher Pa than Pi, Valiparib presented equal values for both, indicating weaker predicted cytotoxic potential compared to the lead compounds. Benzyl butyl phthalate and Ethyl iso-allocholate may exhibit greater predicted cytotoxicity against breast cancer cells than the standard chemotherapeutic agents assessed, thus reinforcing their potential as effective therapeutic candidates, as

initially suggested by molecular docking studies [28]. The more details about the Pa and Pi score of all compounds has been given in Table 3.

Table 3
Comparative analysis of predicted cytotoxic activity (Pa), inactivity (Pi), and inferred apoptotic potential (IAP) of lead OACs—Benzyl butyl phthalate and Ethyl iso-allocholate—in relation to standard breast cancer drugs (Capecitabine and Valiparib) against breast cancer cell lines, as evaluated using the CLC-Pred tool from the PASS online platform.

| Sr.No. | Compounds | Pa | Pi | Cell - line | Description | Tissue/Organ | Tumor type | IAP |
|---|---|---|---|---|---|---|---|---|
| 1. | Benzyl butyl phthalate | 0.312 | 0.044 | Hs-578T | Invasive ductal breast carcinoma | Breast | Carcinoma | 0.268 |
| 2. | Ethyl iso-allocholate | 0.320 | 0.267 | MDA-MB-453 | Breast adenocarcinoma | Breast | Adenocarcinoma | 0.053 |
| 3. | Capecitebine | 0.251 | 0.063 | MDA-MB-361 | Breast adenocarcinoma | Breast | Adenocarcinoma | 0.188 |
| 4. | Valiparib | 0.197 | 0.182 | MDA-MB-361 | Breast adenocarcinoma | Breast | Adenocarcinoma | 0.015 |
| **Condition: Pa > Pi, Pa > 0.3, Pa > 0.7** | | | | | | | | |

## 3. 10 ADMET prediction of potential lead

Solubility in water and absorption profiling of lead compounds are crucial molecular descriptors that provide an adequate number of active molecules in the circulatory system [11]. The solubility in water of Benzyl butyl phthalate predicted − 5.184 (log mol/L) and Ethyl iso-allocholate, − 4.734 (log mol/L). With the lower solubility Benzyl butyl phthalate in compare to Ethyl iso-allocholate, it was suggested as more soluble lead compounds [28]. The Caco-2 permeability of Benzyl butyl phthalate and Ethyl iso-allocholate were predicted to be − 1.569 log Papp in $10^{-6}$ (cm/s), and 1.032 log Papp in $10^{-6}$ (cm/s), respectively. Intestinal absorption in humans is the key parameter for the determination of the bioavailability of compounds (Shukla & Kumar 2024). The tool has predicted the 95.281 absorbed percentage for Benzyl butyl phthalate and 97.702 absorbed percentage for Ethyl iso-allocholate. This showed that the maximum bio-availability was found for the Benzyl butyl phthalate compound.

The distribution pattern of chemicals in different bodily compartments is determined by small compounds because of the separation of the molecules between the bloodstream and the brain tissues [28]. This distribution profiling revealed the blood-brain barrier's (BBB) permeability, which is important for protecting the human CNS (central nervous system). The BBB permeability of these two compounds was predicted to be Benzyl butyl phthalate (0.093 log BB), and Ethyl iso-allocholate (–0.096 log BB). The CNS permeability has been predicted for Benzyl butyl phthalate (–2.249 log PS) and Ethyl iso-allocholate (–2.257 log PS) given in Table 4.

Table 4

ADMET profiling of predicated lead OACs-Benzyl butyl phthalate and Ethyl iso-allocholate of *P. sajor caju* utilized by pkCSM tool by canonical SMILES strings of compounds.

| 1. Absorption | | | | | | | |
|---|---|---|---|---|---|---|---|
| | **Water Solubility** | **Caco-2 Permeability (log Papp in $10^{-6}$ cm/s)** | **Intestinal Absorption (Human) (% Absorbed)** | **Skin Permeability (log Kp)** | **P-glycoprotein Substrate** | **P-glycoprotein I Inhibitor** | **P-glycoprotein II Inhibitor** |
| Benzyl butyl phthalate | -5.184 | 1.659 | 95.281 | -2.673 | Yes | Yes | Yes |
| Ethyl iso-allocholate | -4.734 | 1.032 | 97.702 | -4.057 | Yes | Yes | Yes |
| 2. Distribution | | | | | | | |
| | **VDss (human) (log L/kg)** | **Fraction unbound (human) (Fu)** | **BBB permeability (log BB)** | **CNS permeability (log CS)** | | | |
| Benzyl butyl phthalate | -0.22 | 0 | 0.093 | -2.249 | | | |
| Ethyl iso-allocholate | -0.17 | 0.076 | -0.096 | -2.257 | | | |
| 3. Metabolism | | | | | | | |
| | **CYP2D6 substrate** | **CYP3A4 substrate** | **CYP1A2 inhibitor** | **CYP2C19 inhibitor** | **CYP2C9 inhibitor** | **CYP2D6 inhibitor** | **CYP3A4 inhibitor** |
| Benzyl butyl phthalate | No | Yes | Yes | Yes | Yes | No | No |
| Ethyl iso-allocholate | No | Yes | No | No | No | No | No |
| 4. Excretion | | | | | | | |
| | **Total Clearance (log ml/min/kg)** | | | **Renal OCT2 substrate** | | | |
| Benzyl butyl phthalate | 0.836 | | | No | | | |
| Ethyl iso-allocholate | 0.748 | | | No | | | |
| 5. Toxicity | | | | | | | |
| | **AMES toxicity** | **Max. tolerated dose (human) (log mg/kg/day)** | **hERG I inhibitor** | **hERG II inhibitor** | **Oral Rat Acute Toxicity (LD50) (mol/kg)** | **Oral Rat Chronic Toxicity (LOAEL) (log mg/kg_bw/day)** | **Hepatotoxicity** |
| Benzyl butyl phthalate | No | 1.343 | No | No | 1.934 | 1.45 | No |
| Ethyl iso-allocholate | No | 0.464 | No | No | 0.141 | 1.616 | Yes |

The process by which medications are structurally changed into other molecules in the human liver and intestines by cytochrome P450 enzymes is known as metabolism. It is the primary mechanism influencing the pharmacokinetics (PK) and pharmacodynamics (PD) that establish the safety of the medication. The Benzyl butyl phthalate and Ethyl iso-allocholate

underwent metabolism when a CYP1A2 inhibitor was present. Along with this prediction, Benzyl butyl phthalate was metabolized in presence of CYP2C9 and Ethyl iso-allocholate was metabolized in presence of CPY3A4.

The crucial pharmacological factor that affects the drug's half-life and bioavailability and forecasts the viability of a dosage is the excretion pattern of small molecules. This characteristic serves as the foundation for Figuring out the dosage size [28]. The present study predicted the total clearance of 0.836 in log ml/min/kg and 0.748 in log ml/min/kg was predicted for Benzyl butyl phthalate and Ethyl iso-allocholate respectively. Renal clearance (clearance of drug via kidney) did not find for Benzyl butyl phthalate and Ethyl iso-allocholate.

The maximum dose of these lead compounds that humans may tolerate, according to this toxicity profiling, was estimated to be 1.343 log mg/kg/day for Benzyl butyl phthalate and − 0.596 log mg/kg/day for Ethyl iso-allocholate. “Oral RAT acute toxicity, LD50” determines the lethal dose that cause the 50% death of test organism [11]. was predicted for the Benzyl butyl phthalate (1.934 mol/kg) and Ethyl iso-allocholate (0.141 mol/kg). Benzyl butyl phthalate and Ethyl iso-allocholate were not predicted for hepato-toxic. Benzyl butyl phthalate and Ethyl iso-allocholate were determined to be safe and non-carcinogenic by the computational ADMET prediction for ingestion by humans. Clinical trials were required to verify the efficacy, efficiency, and medication safety of these proposed substances.

## 4. Conclusion

With the findings of present study, *P. sajor-caju* as a promising source of anticancer compounds such as Ethyl iso-allocholate and Benzyl butyl phthalate. Both lead candidates showing strong inhibitory potential against identified hub breast cancer proteins viz. CDKN2A, ERBB2, BRCA1, TP53, ESR1, CDH1, EGF, PTEN, EGFR, and MYC. Their favorable binding affinity, comparable efficacy to standard drugs, and promising pharmacokinetic profiles support their potential as safe and effective candidates for breast cancer therapy.

## Declarations

**Acknowledgement:** We are thankful to the Centre of Biotechnology, University of Allahabad, Prayagraj – 211002, India for proving necessary facilities to carry out this work.

**CRediT authorship contribution statement: Supriya Maurya** Carried out *In silico* work. **Ravi Shanker**: Writing, reviewing **Adarsh Kumar Shuklaand Saba Ehsan** reviewing and editing the manuscript Mohan P. Singh: Conceptualization, guidance, reviewing and editing the manuscript.

**a. Ethics approval and consent to participate:** Not applicable.

**b. Consent for publication:** Not applicable.

**c. Data Availability Statement:**

All data generated or analysed during this study are included in this published article and its supplementary information files.

**d. Declarations of Competing interests:** The authors declare there are no competing interests.

**e. Funding:** This research received no specific grant from any funding agency in the public, commercial, or not-for-profit sectors.

## References

1. Wekking, D., Porcu, M., De Silva, P., Saba, L., Scartozzi, M., & Solinas, C. (2023). Breast MRI: clinical indications, recommendations, and future applications in breast cancer diagnosis. *Current oncology reports*, *25*(4), 257-267. https://doi.org/10.1007/s11912-023-01372-x
2. Sung, H., Ferlay, J., Siegel, R. L., Laversanne, M., Soerjomataram, I., Jemal, A., & Bray, F. (2021). Global cancer statistics 2020: GLOBOCAN estimates of incidence and mortality worldwide for 36 cancers in 185 countries. *CA: a cancer journal for clinicians*, *71*(3), 209-249. https://doi.org/10.3322/caac.21660

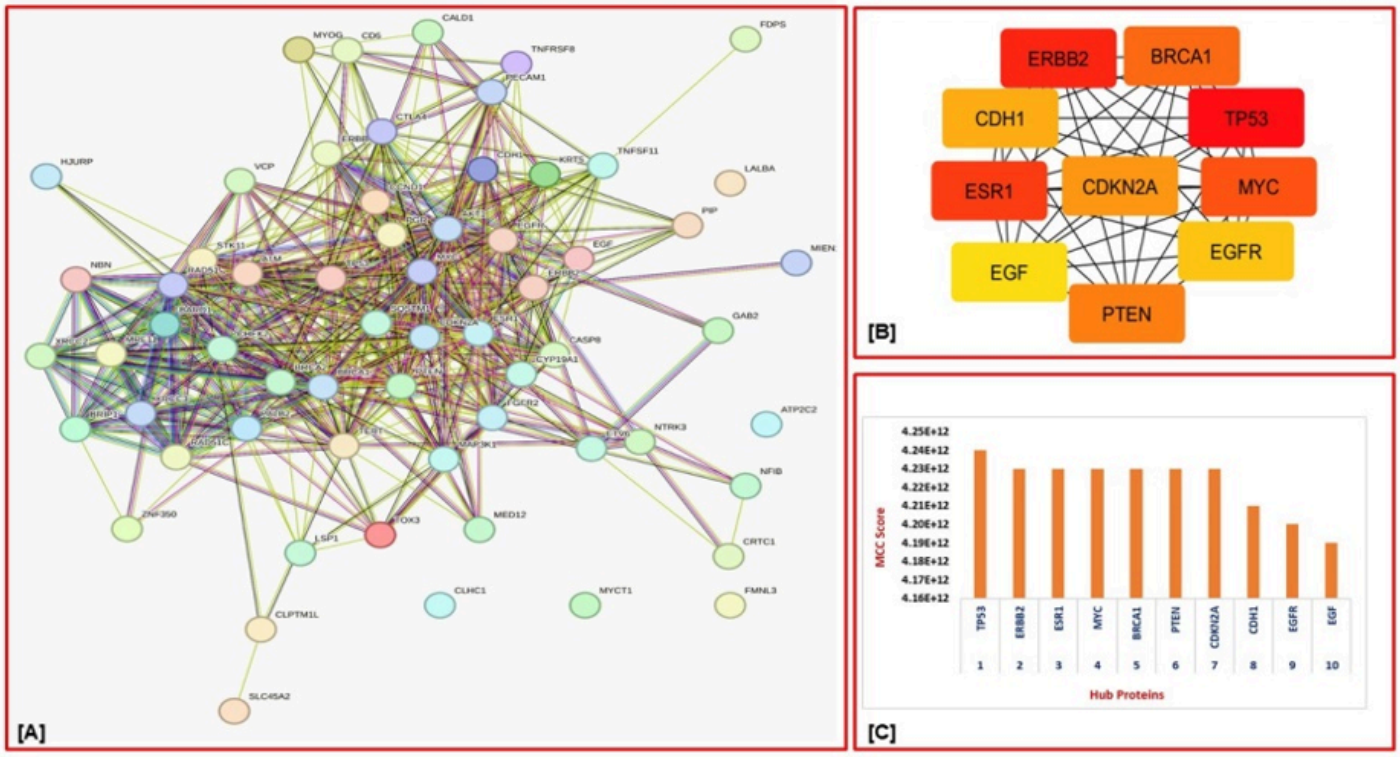
3. Siegel, R. L., Miller, K. D., Fuchs, H. E., & Jemal, A. (2022). Cancer statistics, 2022. *CA: a cancer journal for clinicians*, *72*(1), 7-33. https://doi.org/10.3322/caac.21708
4. Mir, M. A., & Qayoom, H. (2023). Introduction to breast cancer. In *Therapeutic potential of cell cycle kinases in breast cancer* (pp. 1-22). Singapore: Springer Nature Singapore. https://doi.org/10.1007/978-981-19-8911-7_1
5. Liu, L., Tang, Z., Wu, C., Li, X., Huang, A., Lu, X., ... & Xiang, H. (2018). Synthesis and biological evaluation of 4, 6-diaryl-2-pyrimidinamine derivatives as anti-breast cancer agents. *Bioorganic & Medicinal Chemistry Letters*, *28*(6), 1138-1142. https://doi.org/10.1016/j.bmcl.2017.12.066
6. Wang, T., You, Q., Huang, F. S. G., & Xiang, H. (2009). Recent advances in selective estrogen receptor modulators for breast cancer. *Mini Reviews in Medicinal Chemistry*, *9*(10), 1191-1201. https://doi.org/10.2174/138955709789055207
7. Abdullahi, S. H., Uzairu, A., Ibrahim, M. T., & Umar, A. B. (2021). Chemo-informatics activity prediction, ligand based drug design, Molecular docking and pharmacokinetics studies of some series of 4, 6-diaryl-2-pyrimidinamine derivatives as anti-cancer agents. *Bulletin of the National Research Centre*, *45*, 1-22. http://dx.doi.org/10.1186/s42269-021-00631-w
8. Song, C. M., Lim, S. J., & Tong, J. C. (2009). Recent advances in computer-aided drug design. *Briefings in bioinformatics*, *10*(5), 579-591. https://doi.org/10.1093/bib/bbp023
9. Lavecchia, A., & Di Giovanni, C. (2013). Virtual screening strategies in drug discovery: a critical review. *Current medicinal chemistry*, *20*(23), 2839-2860. https://doi.org/10.2174/09298673113209990001
10. Simsek, M., Meijer, B., van Bodegraven, A. A., de Boer, N. K., & Mulder, C. J. (2018). Finding hidden treasures in old drugs: the challenges and importance of licensing generics. *Drug discovery today*, *23*(1), 17-21. https://doi.org/10.1016/j.drudis.2017.08.008
11. Shukla, A. K., & Kumar, A. (2023). Virtual screening of orally active lead compounds of pearl millet and their structural activity against target protein of COVID-19. *Russian Journal of Bioorganic Chemistry*, *49*(Suppl 1), S53-S70. https://doi.org/10.1134/s1068162023080058
12. Usami, A., Nakaya, S., Nakahashi, H., & Miyazawa, M. (2014). Chemical composition and aroma evaluation of volatile oils from edible mushrooms (Pleurotus salmoneostramineus and P. sajor-caju). *Journal of Oleo Science*, *63*(12), 1323-1332. https://doi.org/10.5650/jos.ess14147
13. Singh, M. P., Rai, S. N., Dubey, S. K., Pandey, A. T., Tabassum, N., Chaturvedi, V. K., & Singh, N. B. (2022). Biomolecules of mushroom: A recipe of human wellness. *Critical Reviews in Biotechnology*, *42*(6), 913-930. https://doi.org/10.1080/07388551.2021.1964431
14. Rathore, H., Prasad, S., & Sharma, S. (2020). Screening of Bioactive Compounds of P. sajor-caju Extracted Using Supercritical CO2 Fluid Extraction Technique. In *Emerging Technologies in Food Science: Focus on the Developing World* (pp. 239-246). Singapore: Springer Singapore. https://doi.org/10.1007/978-981-15-2556-8_21
15. Saad, W. Z., Hashim, M., Ahmad, S., & Abdullah, N. (2014). Effects of heat treatment on total phenolic contents, antioxidant and anti-inflammatory activities of P. sajor-caju extract. *International Journal of Food Properties*, *17*(1), 219-225. https://doi.org/10.1080/10942912.2011.619290
16. Krümmel, A., Rodrigues, L. G. G., Vitali, L., & Ferreira, S. R. S. (2022). Bioactive compounds from P. sajor-caju mushroom recovered by sustainable high-pressure methods. *Lwt*, *160*, 113316. https://doi.org/10.1016/j.lwt.2022.113316
17. Rossi, P., Difrancia, R., Quagliariello, V., Savino, E., Tralongo, P., Randazzo, C. L., & Berretta, M. (2018). B-glucans from Grifola frondosa and Ganoderma lucidum in breast cancer: an example of complementary and integrative medicine. *Oncotarget*, *9*(37), 24837. https://doi.org/10.18632/oncotarget.24984
18. Jiang, J., & Sliva, D. (2010). Novel medicinal mushroom blend suppresses growth and invasiveness of human breast cancer cells. *International journal of oncology*, *37*(6), 1529-1536. https://doi.org/10.3892/ijo_00000806
19. Joseph, T. P., Chanda, W., Padhiar, A. A., Batool, S., LiQun, S., Zhong, M., & Huang, M. (2018). A preclinical evaluation of the antitumor activities of edible and medicinal mushrooms: A molecular insight. *Integrative cancer therapies*, *17*(2), 200-209. https://doi.org/10.1177/1534735417736861
20. Dowaraka-Persad, B., & Neergheen, V. S. (2023). Mushroom-derived compounds as metabolic modulators in cancer. *Molecules*, *28*(3), 1441. https://doi.org/10.3390/molecules28031441

21. Panda, S. K., & Luyten, W. (2022). Medicinal mushrooms: Clinical perspective and challenges. *Drug Discovery Today*, *27*(2), 636-651. https://doi.org/10.1016/j.drudis.2021.11.017
22. Gariboldi, M. B., Marras, E., Ferrario, N., Vivona, V., Prini, P., Vignati, F., & Perletti, G. (2023). Anti-cancer potential of edible/medicinal mushrooms in breast cancer. *International journal of molecular sciences*, *24*(12), 10120. https://doi.org/10.3390/ijms241210120
23. Mishra, D., Mishra, A., Nand Rai, S., Vamanu, E., & Singh, M. P. (2023). Demystifying the role of prognostic biomarkers in breast cancer through integrated transcriptome and pathway enrichment analyses. *Diagnostics*, *13*(6), 1142. https://doi.org/10.3390/diagnostics13061142
24. Kandasamy, S., Chinnappan, S., Thangaswamy, S., Balakrishnan, S., & Khalifa, A. Y. (2020). Assessment of antioxidant, antibacterial activities and bioactive compounds of the wild edible mushroom Pleurotus sajor-caju. International Journal of Peptide Research and Therapeutics, 26(3), 1575-1581.
25. Gülmez, Ö., Özdal, M., Algur, Ö. F., & Yilmaz, B. (2021). Determination of chemical constituents and bioactive properties of alcohol extracts of Pleurotus sajor-caju and Pleurotus ostreatus. Journal of the Institute of Science and Technology, 11(3), 1734-1741.
26. Mishra, D., Mishra, A., & Singh, M. P. (2022). *In silico* insight to identify potential inhibitors of BUB1B from mushroom bioactive compounds to prevent breast cancer metastasis. *bioRxiv*, 2022-06. https://doi.org/10.31083/j.fbl2807151
27. Shukla, A. K., & Kumar, A. (2024). Comparative study between antiviral drugs and natural compounds against “Cryo-EM structure of the SARS-CoV-2 Omicron spike”. *Vegetos*, *37*(2), 596-605. https://doi.org/10.1007/s42535-023-00690-6
28. Shukla, A. K., & Kumar, A. (2025). A chemoinformatics study to prioritization of anticancer orally active lead compounds of pearl millet against adhesion G protein-coupled receptor. *Spectrochimica Acta Part A: Molecular and Biomolecular Spectroscopy*, *334*, 125960 https://doi.org/10.1016/j.saa.2025.125960
29. Mishra, V., Tripathi, V., Yadav, P., & Singh, M. P. (2023). Beta glucan as an immune stimulant in tumor microenvironment—Insight into lessons and promises from past decade. *International Journal of Biological Macromolecules*, *234*, 123617. https://doi.org/10.1016/j.ijbiomac.2023.123617
30. Singh, M. P., Singh, N., Mishra, D., Ehsan, S., Chaturvedi, V. K., Chaudhary, A., ... & Vamanu, E. (2023). Computational approaches to designing antiviral drugs against COVID-19: a comprehensive review. *Current Pharmaceutical Design*, *29*(33), 2601-2617. https://doi.org/10.2174/0113816128259795231023193419
31. Jha, R. K., Shukla, A. K., Kumari, A., & Kumar, A. (2024). Virtual screening of potential orally active anti-bacterial compounds of finger millet. *Vegetos*, 1-12. https://doi.org/10.1007/s42535-024-01051-7
32. Vishal, Banyal, S., Shukla, A. K., Kumari, A., Kumar, A., Khatak, A., & Kumar, M. (2023). Effect of modification on Quality Parameters of Jackfruit (Atrocarpus heterophyllus) seed starch to valorize its food potential and In-Silico Investigation of the pharmacological compound against salmonellosis. *Waste and Biomass Valorization*, *14*(5), 1597-1610. https://doi.org/10.1007/s12649-022-01945-0
33. Lagunin, A. A., Rudik, A. V., Pogodin, P. V., Savosina, P. I., Tarasova, O. A., Dmitriev, A. V., ... & Poroikov, V. V. (2023). CLC-Pred 2.0: a freely available web application for *In silico* prediction of human cell line cytotoxicity and molecular mechanisms of action for druglike compounds. *International Journal of Molecular Sciences*, *24*(2), 1689. https://doi.org/10.3390/ijms24021689
34. Bashari, M. H., Huda, F., Tartila, T. S., Shabrina, S., Putri, T., Qomarilla, N., ... & Meiyanto, E. (2019). Bioactive compounds in the ethanol extract of marine sponge Stylissa carteri demonstrates potential anti-cancer activity in breast cancer cells. Asian Pacific journal of cancer prevention: APJCP, 20(4), 1199. https://doi.org/10.31557/apjcp.2019.20.4.1199
35. Zhang, J., Yan, Z., Wang, Y., Wang, Y., Guo, X., Jing, J., ... & Wu, C. (2021). Cancer-associated 53BP1 mutations induce DNA damage repair defects. *Cancer Letters*, *501*, 43-54. https://doi.org/10.1016/j.canlet.2020.12.033
36. Fidyt, K., Fiedorowicz, A., Strządała, L., & Szumny, A. (2016). β-caryophyllene and β-caryophyllene oxide—natural compounds of anticancer and analgesic properties. *Cancer medicine*, *5*(10), 3007-3017. https://doi.org/10.1002/cam4.816
37. Schotanus, M. D., & Van Otterloo, E. (2020). Finding MEMO—emerging evidence for MEMO1' s function in development and disease. *Genes*, *11*(11), 1316. https://doi.org/10.3390/genes11111316
38. Pande, K., Bettadaiah, B. K., & Kannan, A. (2024). A biocompatible nanoformulation of curcumin analogue and curd exosomes targeting EphA2 signalling cascade in head and neck cancer. *Cancer Nanotechnology*, *15*(1), 50.

https://doi.org/10.1186/s12645-024-00286-y

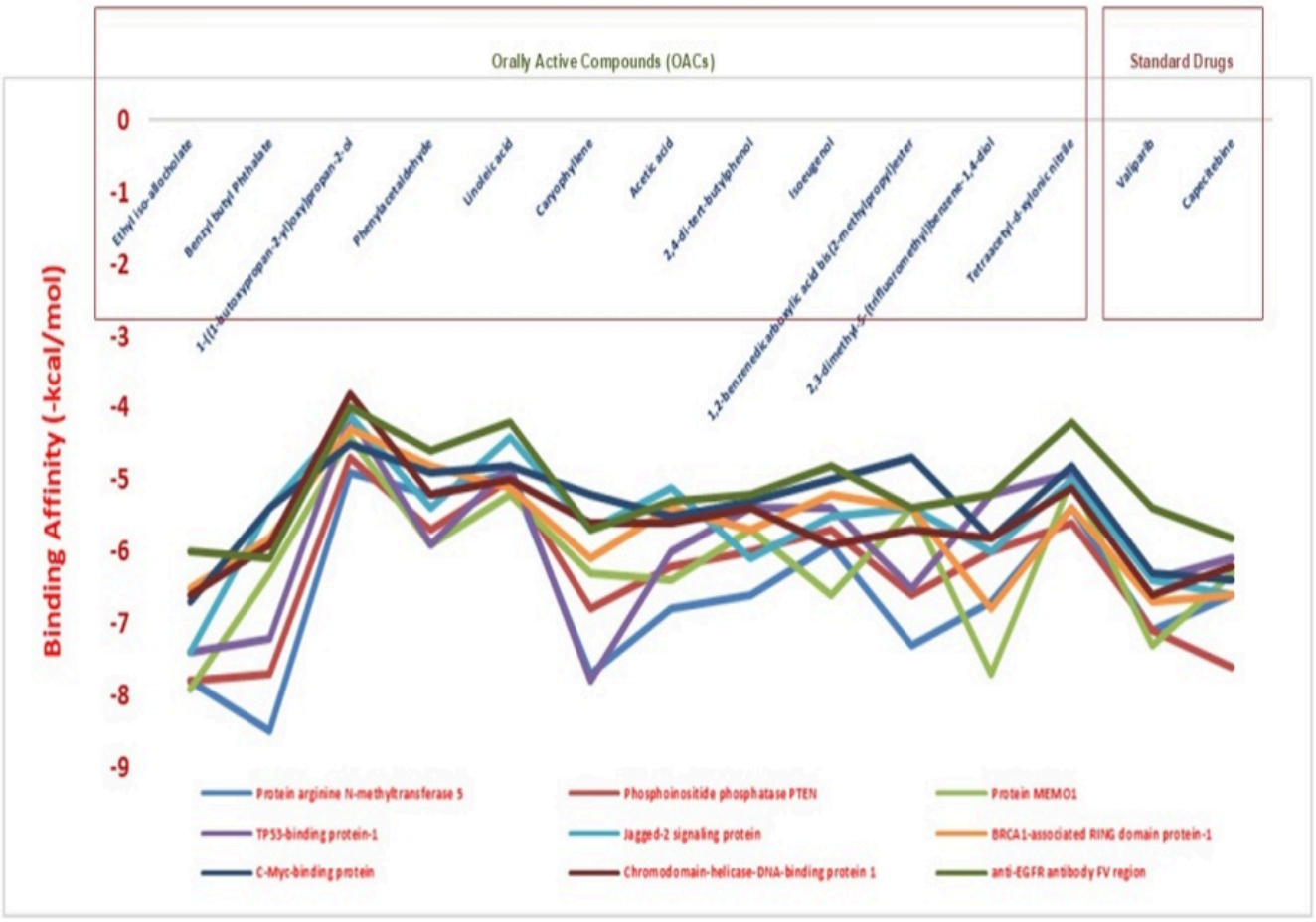
39. Ariyannur, P., & Srinivasalu, V. K. (2020). Early Breast Cancer. *Management of Early Stage Breast Cancer: Basics and Controversies*, 59. https://doi.org/10.1007/978-981-15-6171-9_5
40. Al-Gara, awi, N. I., Abu-Serag, N. A., Alee Shaheed, K. A., & Bahadly, Z. K. A. (2019, August). Analysis of bioactive phytochemical compound of (Cyperus alternifolius L.) by using gas chromatography–mass spectrometry. In *IOP conference series: Materials science and engineering* (Vol. 571, p. 012047). IOP Publishing. http://dx.doi.org/10.1088/1757-899X/571/1/012047
41. Kumar, K. S., Jyothi, M. N., & Prashant, A. (2025). CHD1 dysregulation in cancer: bridging chromatin instability, therapy resistance, and immune evasion. *Molecular Biology Reports*, *52*(1), 1-14. https://doi.org/10.1007/s11033-025-10536-w
42. Han, T., Jiang, S., Zheng, H., Yin, Q., Xie, M., Little, M. R., ... & Wan, L. (2019). Interplay between c-Src and the APC/C co-activator Cdh1 regulates mammary tumorigenesis. *Nature Communications*, *10*(1), 3716. https://doi.org/10.1038/s41467-019-11618-7
43. Burgel, P. R., & Nadel, J. A. (2008). Epidermal growth factor receptor-mediated innate immune responses and their roles in airway diseases. *European Respiratory Journal*, *32*(4), 1068-1081. https://doi.org/10.1183/09031936.00172007
44. Feng, Y., Dai, X., Li, X., Wang, H., Liu, J., Zhang, J., ... & Xia, L. (2012). EGF signalling pathway regulates colon cancer stem cell proliferation and apoptosis. Cell proliferation, 45(5), 413-419. https://doi.org/10.1111/j.1365-2184.2012.00837.x
45. Chakraborty, B., Byemerwa, J., Krebs, T., Lim, F., Chang, C. Y., & McDonnell, D. P. (2023). Estrogen receptor signaling in the immune system. *Endocrine reviews*, *44*(1), 117-141. https://doi.org/10.1210/endrev/bnac017
46. Hegab, M. H., Abdelhameed, M. S., Shawer, E. E., El-Dein, A. N., Sabour, R., & Ghareeb, M. A. (2024). Chemical constituents of ostracod Heterocypris salina extract, anticancer and antimicrobial activity: *In silico* supported in vitro study. *Egyptian Pharmaceutical Journal*, *23*(1), 85-93. https://doi.org/10.4103/epj.epj_107_23
47. Sicińska, P. (2019). Di-n-butyl phthalate, butylbenzyl phthalate, and their metabolites exhibit different apoptotic potential in human peripheral blood mononuclear cells. *Food and Chemical Toxicology*, *133*, 110750. https://doi.org/10.1016/j.fct.2019.110750
48. Khamn, S., Thakur, A. K., & Singh, K. J. (2023). Phytochemical screening and its relevance in Hemiphragma heterophyllum Wall., a medicinally important plant from Shimla hills. *Medicinal Plants-International Journal of Phytomedicines and Related Industries*, *15*(1), 116-123. https://doi.org/10.5958/0975-6892.2023.00011.4

## Figures




## Figure 1

Illustrative representation of [A] comprehensive protein-protein interaction (PPI) network of CHD targets using the STRING database, [B] a CytoHubba analysis for ranking calculation, top 10 essential nodes by MCC scores network, and [C] node and edge annotations are accessible through Cytoscape Data Panel.




## Figure 2

Graph showing the binding affinities (-kcal/mol) between OACs of mushroom bioactive and prioritized ranked hub genes, obtained using blind docking with PyRx and confirmed with AutoDock Vina platform.

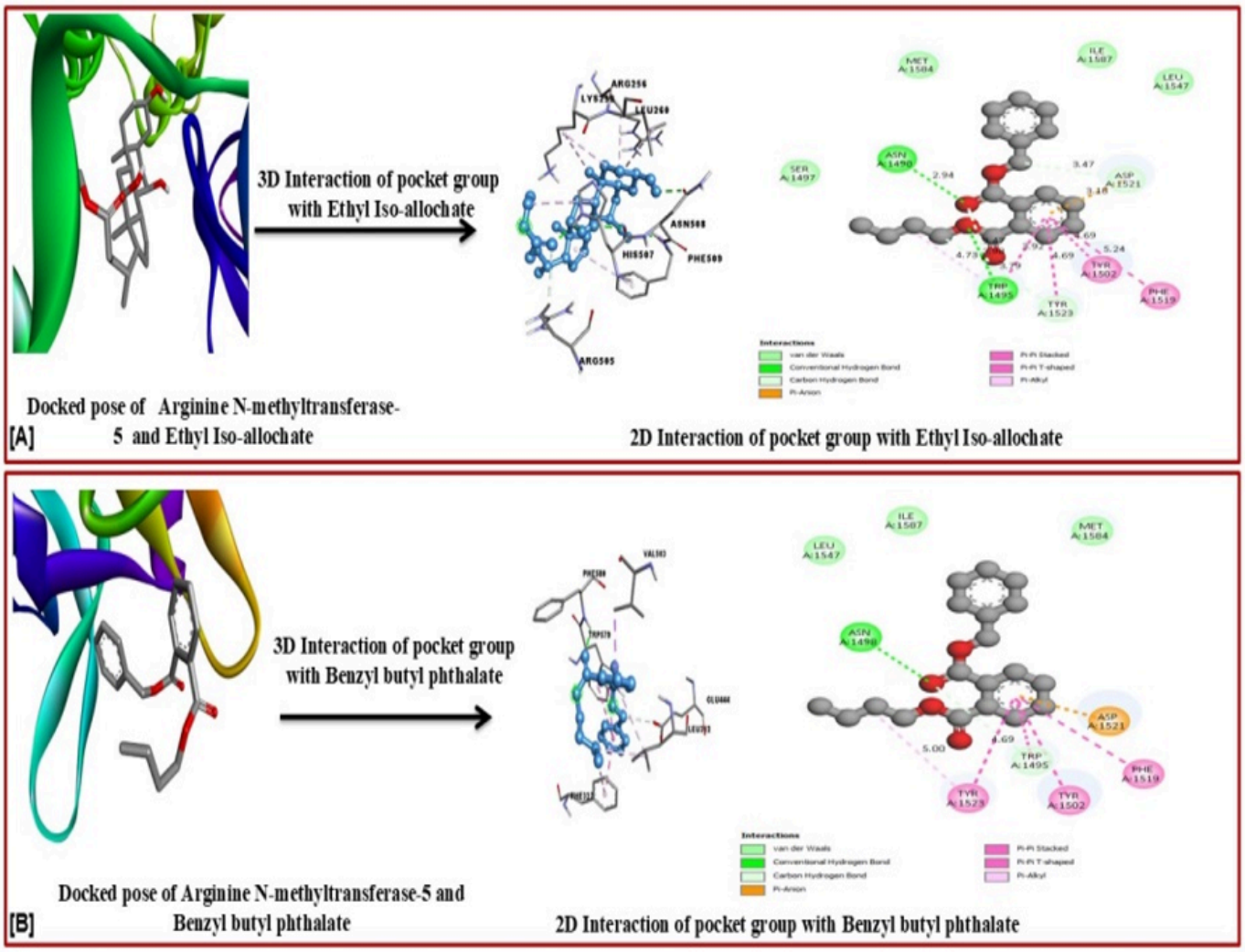
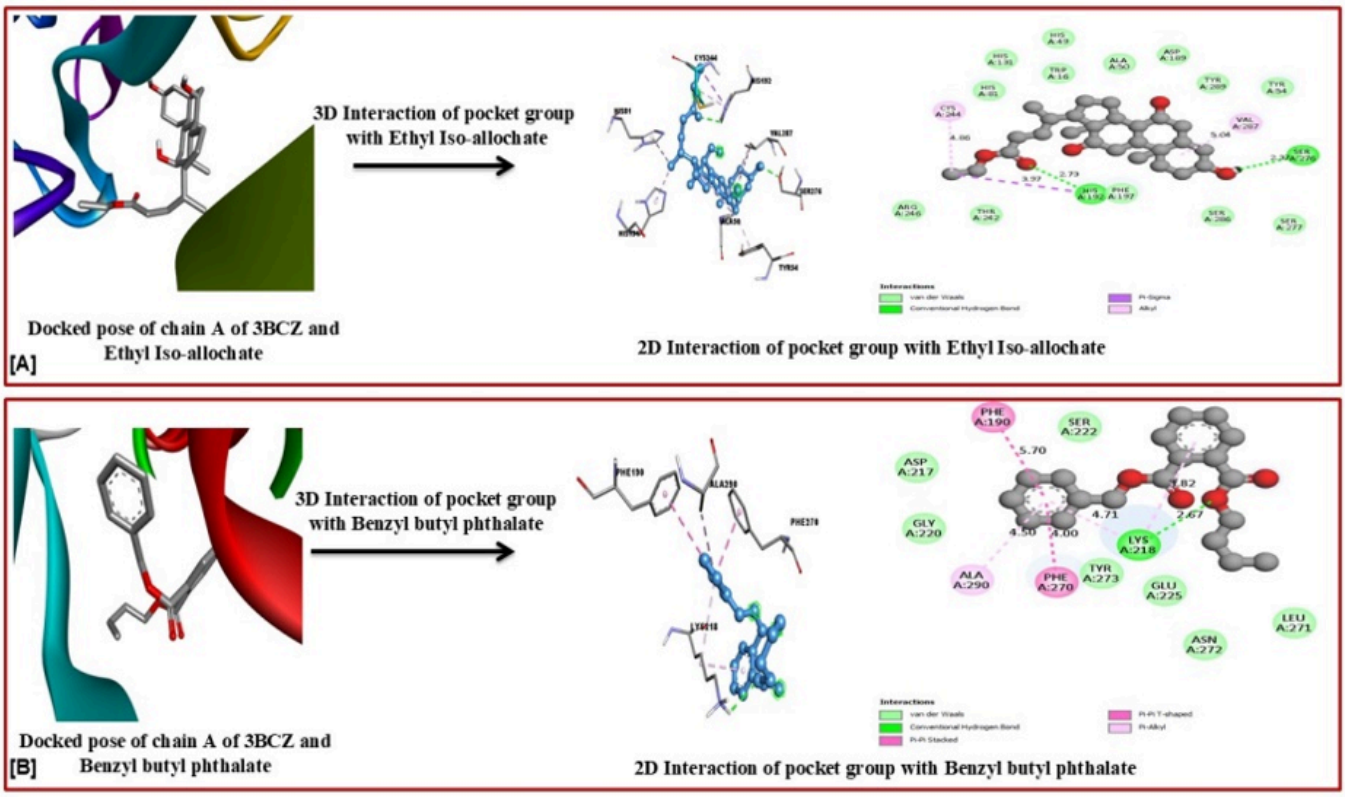



Figure 3

Illustration of three-dimensional docked pose and binding pattern of [A] Arginine N-methyltransferase-5 and Ethyl Iso-allochate, and [B] Benzyl butyl phthalate utilized by BIOVIA Discovery Studio.




## Figure 4

Illustration of three-dimensional docked pose and binding pattern of a target protein [A] protein MEMO1 and Ethyl iso-allocholate, and [B] Benzyl butyl phthalate utilized by BIOVIA Discovery Studio.

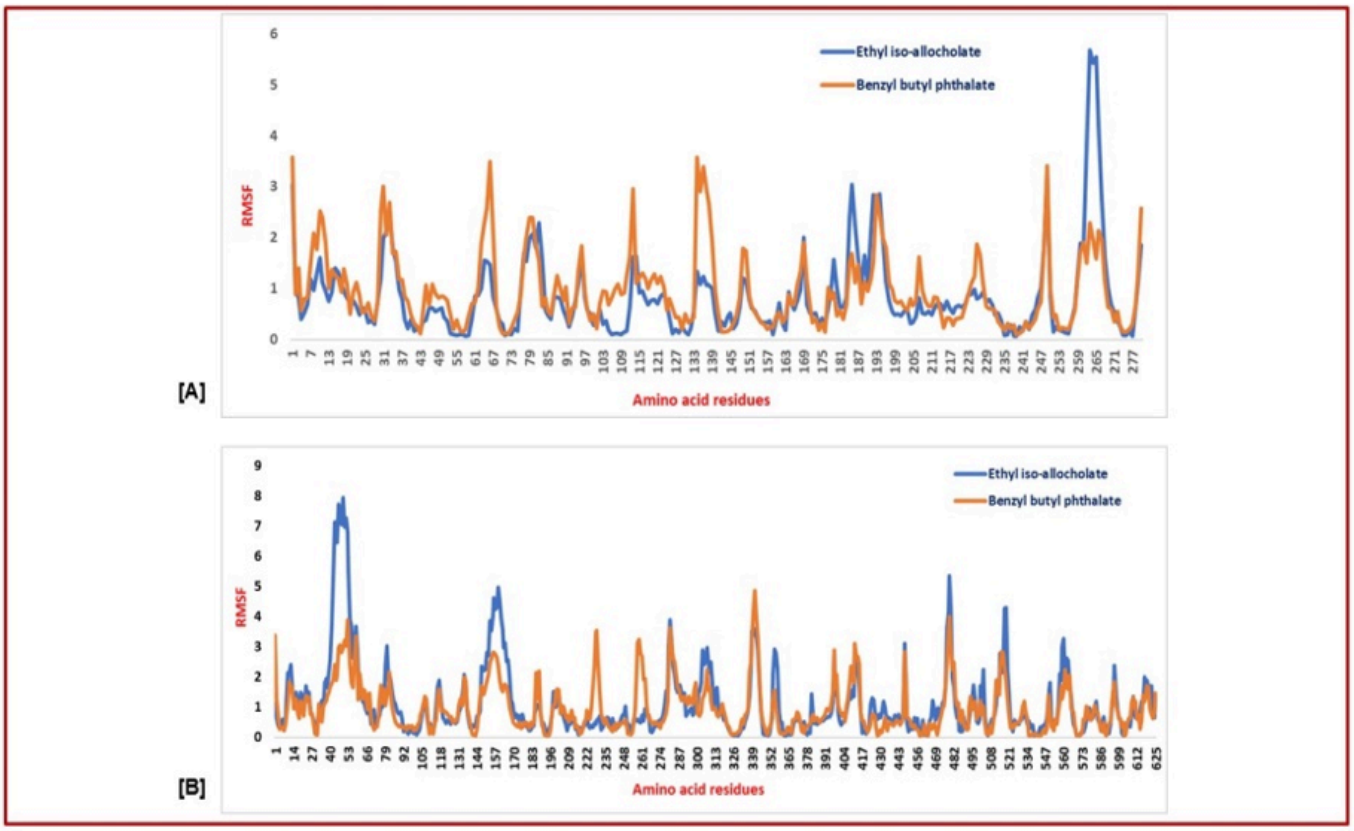


**Figure 5**

Illustration of root mean square fluctuations of [A] docked pose of protein MEMO-1 with Ethyl iso-allocholate and Benzyl butyl phthalate [B] docked pose of arginine N-methyltransferase-5 with Ethyl iso-allocholate and Benzyl butyl phthalate in default parameters of CABS Flex server such as protein rigidity: 1.0, number of cycles: 50, cycle between trajectory: 50 for the 10 nano second.

## Supplementary Files

This is a list of supplementary files associated with this preprint. Click to download.

- SupplementaryMaterials.docx
- GraphicalAbstract.docx